

## Sedimentology and Geochemistry of Quaternary Coastal Sediments of Alappuzha District, Kerala, Southwest India: Implications on Coastal Evolution

Akash Padmalal<sup>1\*</sup>, Padmalal Damodaran<sup>2</sup>, Vishnu S. Mohan<sup>3</sup> and Deepak M. Maurya<sup>4</sup>

<sup>1</sup>Department of Geology and Environmental Science, Christ College, Irinjalakuda-680125(KL), India

<sup>2</sup>Formerly with National Centre for Earth Science Studies, Thiruvananthapuram-695011(KL), India

<sup>3</sup>Department of Geology, Sree Narayana College, Sivagiri, Varkala-695145(KL), India

<sup>4</sup>Department of Geology, The M. S. University of Baroda, Vadodara-390002(GJ), India

(\*Corresponding Author, E-mail:akash.padmalal47@gmail.com, ORCID: 0000-0001-7919-3068)

### Abstract

The coastal areas are the most dynamic and strategic regions of the world that are under constant threat due to climate and sea level changes. Further, these are densely populated regions undergoing rapid socio-economic development. Hence, information on the coastal environments and their sediment characteristics (surface and subsurface) is very crucial not only for planning future developments but also for mitigating the impact of anthropogenic activities on this crucial ecosystem in the land-sea interface. Among the coastal environments of the world, the southwestern coast of India received special attention because of its outstanding natural beauty and occurrence of economically viable placer mineral resources. The region acts as a "Gate way of Indian Summer Monsoon (ISM)". However, the lack of adequate information on the subsurface sediment characteristics and paleoenvironmental potential is a major setback for the planning sustainable development framework for the region. Here we report the sedimentological and geochemical characteristics of a 30 m-long borehole core retrieved from the coastal area of the Alappuzha, which is covered by a thick layer of Cenozoic sediments. The sediment textural analysis indicates that the upper 14.7 m of the borehole core contains moderately sorted, medium to coarse sand, overlying a poorly sorted, organic carbon-rich, silty clay with broken and complete shells. The microfauna in the borehole sediments include *Ammonia*, *Bolivina*, and *Virgulina* indicating a shallow marine/lagoonal environment that prevailed during the deposition of the finer clastics in the borehole site. Cluster analysis of the geochemical parameters shows that the SiO<sub>2</sub> content behaves as a lone member exhibiting a negative correlation with all the other major and trace elements except for the element Zr which occurs mainly in the form of the mineral zircon (ZrSiO<sub>4</sub>) in the coarser sediments. The ternary plot, CM diagram, and the SiO<sub>2</sub>/Al<sub>2</sub>O<sub>3</sub> ratio indicate that the texturally mature quartz sand in the upper level was deposited under a high-energy (shoreface) environment, whereas the lower silty clay sediments under a comparatively calm (shallow marine-lagoon) environment. These results suggest that the sedimentary framework of the region has been developed from a shallow coastal embayment due to the progradation of sand dominant sediments brought by the longshore currents.

**Keywords:** Coastal Sediments, Coastal Geomorphology, Sediment Texture, Major and Trace Elements, Coastal Evolution

### Introduction

Coastal areas where the land and sea meet are some of the most dynamic regions of the earth that are under the constant interactions of natural and anthropogenic processes (Kumar *et al.*, 2023; Bagul *et al.*, 2025; Bhatnagar *et al.*, 2025). The sediments in this zone have a special capability to dissipate the fury of the sea waves through its different types of sediment transport mechanisms - traction, saltation, and suspension (Hanamgond *et al.*, 2017; Pradhan *et al.*, 2020), thereby protecting the coastal lands from sea erosion. The sea level oscillations and climate changes play a pivotal role in the making up of the coastal environments. Being a densely populated region hosting most of the developmental

centers, the coastal environments receive excessive input of nutrients, heavy metals and other pollutants from point and non-point sources which will adversely affect the ecosystem structure and functions in the long run (Vikas and Dwarakish, 2015; Danovaro and Boero, 2019, Chakraborty *et al.*, 2022). Therefore, the environment requires constant monitoring and mitigation measures to maintain the health of this crucial ecosystem that connect the land and the sea/ocean.

Sedimentology and geochemistry of subsurface coastal sediments provide a wealth of information on the nature and characteristics of the deposits. The data base can also be used for unravelling the paleoclimate and paleoenvironmental conditions that prevailed during the deposition of sediments (Cui *et al.*, 2016). The sedimentary archives of the coastal area often embed evidences of human habitation and maritime trades as well (Cherian *et al.*, 2012, Das *et al.*, 2024). Coastal sediments of many tropical coasts

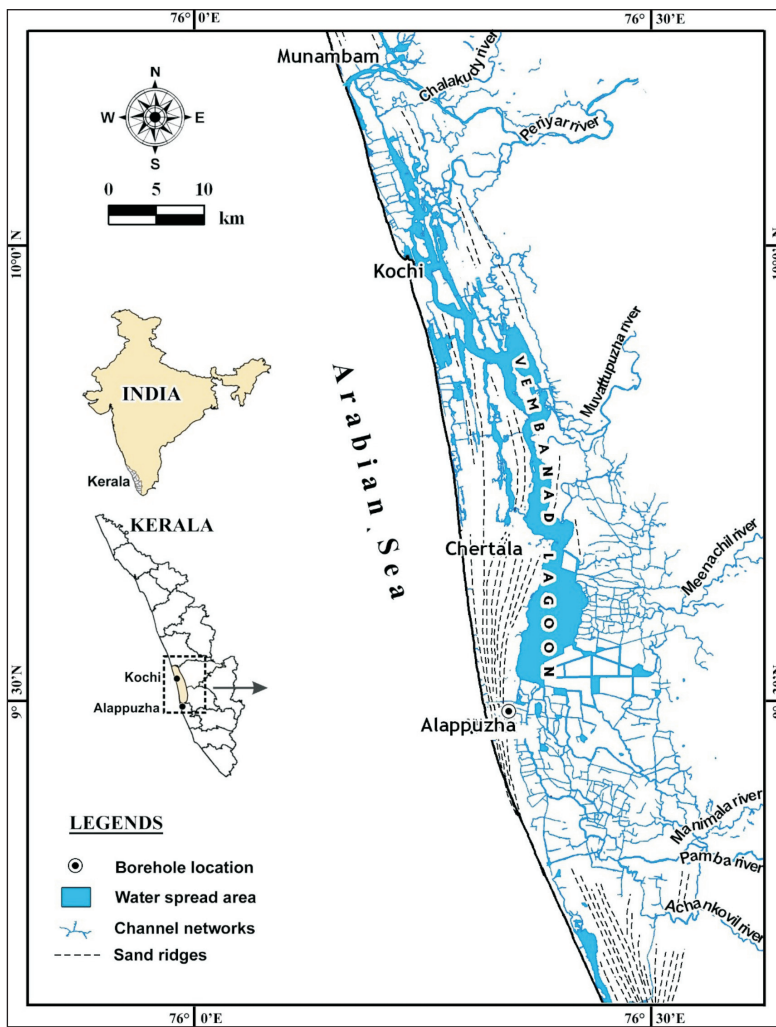


**Fig.1.** Vembanad Lagoon and adjoining regions. Note the location of the borehole used for the present study

contain many mechanically segregated minerals of strategic importance and Kerala coast in southwest India is an example as it contains economically viable placer mineral deposits like ilmenite, rutile, monazite etc. (Soman, 2002).

The Kerala state in southwest India has a 590 km-long coastal line, of which 360 km shows dynamic changes in terms of erosion and deposition of sediments (Narayanan and Priju, 2006). The occurrence of lakes and lagoons with their inflowing rivers, ridge-runnel systems and barrier beaches separating the backwaters from the sea are evidence of the prograding nature of the coast during the last interglacial (Narayanan and Priju, 2006). Among the coastal backwater bodies, the Vembanad Lake is the largest one and is a Ramsar wetland of international importance. The region coincides with the central part of the South Kerala Sedimentary Basin (SKSB) where the maximum thickness of Cenozoic sediments is reported (Nair et al., 2006). Previous studies revealed that the Vembanad Lake has been evolved from an embayment of the sea through the progressive growth of a sand bar (Padmalal et al., 2014a). Although a wealth of information exists on the biological and water quality aspects of the lagoon and its adjoining regions (Sajeev et al., 2020; Sundar and Kundapura, 2023; Joseph and Gandhi, 2025) detailed sedimentological and geochemical aspects of subsurface sediments of the barrier beach/strand plain system is meagre. Therefore, in the present study an attempt has been made with the aim of

understanding the sedimentological and geochemical characteristics of a 30 m long borehole core retrieved from the barrier beach at Alappuzha ( $09^{\circ}29'35''N$ ,  $76^{\circ}20'24''E$ ; Fig. 1).

### Study Area and Subsurface Geology

The borehole core used in the present study was retrieved from the beach- strandplain system of the Alappuzha coast, (Alappuzha district) in Kerala state (SW India). The core site is located about 2.5 km inland of the present coastline and is close to the western bank of the Vembanad Lagoon (Fig. 1). The coastal district of Alappuzha is the smallest district which constitutes only 3.64% of the total area of the Kerala state. The district is known for many discrete water bodies of variable dimensions, the largest of which is the southern Vembanad Lagoon. The Kuttanad Kole wetland is the silted-up part of the Vembanad Lagoon that existed prior to Late Holocene (Maya et al., 2022; Shaji et al., 2022). Vembanad Lagoon is the largest backwater system in the west coast of India with a length of about 96 km and water spread area of about  $230 \text{ km}^2$ . The lagoon is separated from the Arabian Sea by a coastal barrier which is interrupted at two places, one at Fort Kochi and the other at Munambam. The width of the lagoon varies from a few hundred meters to about 4.5 km (Maya et al., 2007). The maximum width of the lagoon is at its southern end, where 4 important rivers,

the Achankovil, Pamba, Mammala and Meenachil, discharge into the lagoon. The Chalakudy and Periyar rivers reach the Vembanad Lagoon from its northern end, while the Muvattupuzha River reaches the middle of the lagoon. The lagoon water becomes brackish to nearly fresh during the Monsoon season (Nasir and Harikumar, 2012).

The Alappuzha district is essentially a sandy strip of land separated by water bodies. The district comprises two broad physiographic zones of Kerala; the lowlands (< 8m above msl) and the midlands (8 - 75m above msl) (KSLUB, 1995; CESS, 1984). The district has a relatively flat topography (Mareena and Prasad, 2020), except for isolated hillocks that form part of the midlands and occur on its southeastern part. The lowlands with sand dunes and backwaters form a considerable portion (~ 80%) of the district. Coastal plains with lagoons, including Vembanad Lagoon, are important physiographic units of the lowlands. Most of the coastal plains show topographic relief between 4 m and 6 m above msl. This zone comprises a variety of landform features with unique characteristics, including dunes, ancient beach ridges, barrier flats, coastal alluvial plains, floodplains, rivers, river terraces, marshes, and lagoons. The present borehole core is retrieved from a beach-strand plain system of the Alappuzha coast (Fig. 1).

Geologically, the study area coincides with the deepest portion of the SKSB- landward extension of the Kerala-Konkan basin (Nair *et al.*, 2006). The thickness of the sediments overlying the basement of Archaean crystalline rocks reaches up to ~ 700m, near Alappuzha (~ 600m of Neogene sediments and 100m of late Quaternary sediments) (Nair and Rao, 1980; Nair *et al.*, 2006; Padmalal *et al.*, 2014a). The Neogene sediments comprise the Vaikom, Quilon and Warkalli Formations (Table 1). The late Quaternary sediments consist of coastal sands and lagoonal clays with broken and complete shells (Padmalal *et al.*, 2014a). Fig. 2 shows the geology of the Vembanad Lagoon catchments and its adjoining areas (Soman, 2002). The area experiences a warm humid climate with a general temperature variation of 28-32°C. The study area receives average annual rainfall of 2,500 mm, out of this 70% is derived from the southwest monsoon and the remaining (~28%) from the NE monsoon and summer showers (2%).

## Material and Methods

The borehole core used for the present study was collected from the paleo strandline of the Alappuzha coast by rotary drilling method. The split sediment sampler fixed at the free end of the drilling rod lifts 45 cm long undisturbed sediment at specified depths. The sampler is fully lined by PVC in order to avoid contamination from the metallic body of the split sediment sampler. The subsamples of the core from selected depths (adequately representing the different litho-units) were oven dried at 55+ 3°C and is used for further analysis. Extreme care was taken to avoid contamination while handling the samples. A total of 18 samples are used for textural studies and 9 samples are used for elemental analysis and extraction studies.

## Sedimentological and Heavy Mineralogical Studies

Textural analyses were carried out on original dried subsamples following combined sieving and pipette analysis method of Lewis (1984). The sand fraction was sieved at half phi interval on a Ro-Tap sieve shaker and the weight percentages of the

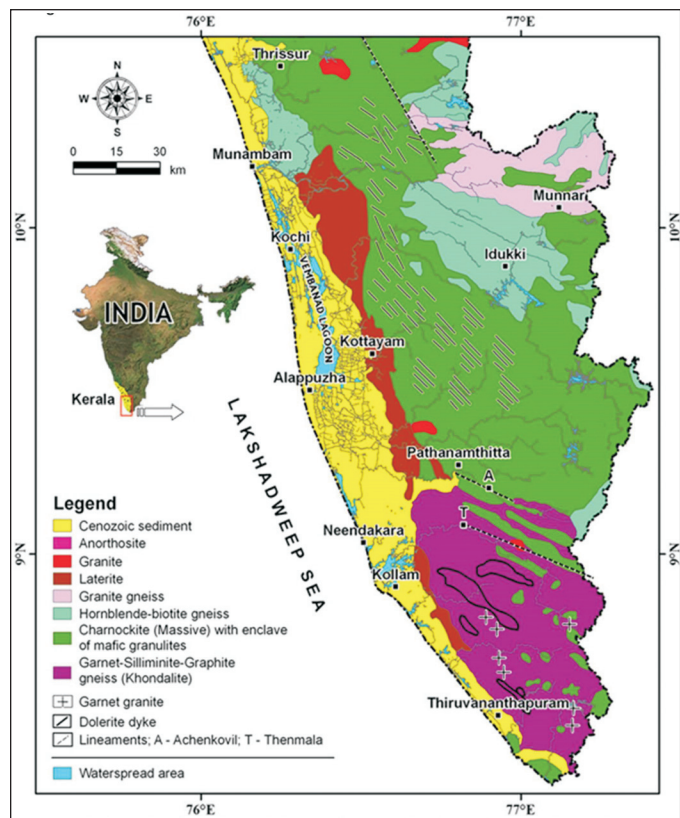


**Fig.2.** Geology of hinterlands of the Vembanad lagoon and nearby area (source: Soman, 2002)

fractions retained in each sieve were calculated. The statistical parameters such as Mean, Standard deviation (Sediment sorting), Skewness and Kurtosis were determined using the graphical method of Folk and Ward (1957). The different equations used for these computations are given in Table 2. The fine sand fraction from selected subsamples were separated into heavy and light mineral fractions using bromoform separation method (Carter, 1974). The heavy minerals mounted on glass slides and mineral species were identified using petrographical microscope following Mange and Maurer (1992). A total of about 300 grains were counted to find out the number percentages of the individual minerals. The major microfossils in the coarser fraction were separated out and well

**Table 1:** Stratigraphy of Kerala (*Modified after* Najeeb, 1999)

Quaternary	Vembanad Formation	Sand, clays, molluscan shell beds, riverine alluvium and floodplain deposits. Laterite capping the crystalline rocks and Neogene sediments.
Neogene	Warkalli Formation	Sandstone and clay with lignite seams
	Quilon Formation	Limestone, marls, clays/calcareous clays with marine and lagoon fossils.
	Vaikom Formation	Sandstone with pebbles and gravel beds, clays and lignite and carbonaceous clay.
Unconformity		
Archaeon to Mesozoic	Intrusives: Veins of quartz, pegmatites, Mesozoic granites, granophyres, dolerite and gabbro Garnet sillimanite gneiss, hornblende-biotite gneiss, garnet-biotite gneiss, quartz-feldspathic gneiss, charnockites, charnockite gneiss etc.	

cleaned with distilled water and air dried at low temperature and subjected to Scanning Electron Microscopic (SEM) analysis (Hitachi SU1510).

### Geochemical Studies

A portion of the bulk sample was finely powdered and homogenized using an agate mortar for geochemical studies. The organic carbon in the sediments were estimated following wet oxidation method of Jackson *et al.*, (1950) using chromic acid as an oxidizing medium and diphenyl amine as indicator. The values not differing 0.2% of the analysis was used in this study. The major and trace element geochemistry of the sediments were carried out by two approaches:

1) X-Ray fluorescence method: The finely powdered samples were combusted in a muffle furnace at ~950°C and loss on ignition (LOI) was estimated (Hackenson and Jansson, 1983). After LOI, samples were pelletized as per standard procedures and then fed into XRF machine. A Bruker model S4 Pioneer sequential wave dispersive X-Ray Spectrometer equipped with a goniometer (4 kW Rh X-Ray tube) available at the National Center for Earth Science Studies (NCESS), Thiruvananthapuram, Kerala, India is used to measure the major and trace element contents in the core samples. JMs-1 (marine sediment, Geological Survey of Japan) is used as reference standard material for checking the accuracy and reproducibility of the analysis and the measured concentrations are within the range of certified values. 2) Ammonium acetate extraction method: Coastal areas are the sinks of particulate materials derived from both terrestrial and near shore/ offshore marine environments. The cations like alkali (Na, K) and alkaline earth (Ca, Mg) are dominant elements that play a pivotal role in the geochemistry of sediments and interstitial waters of the subsurface deposits in the coastal area. Out of the different phases of element association in sediments such as exchangeable, organic bound, Fe-Mn oxide bound and lattice bound forms, the exchangeable cations received much attention (Gupta and Chen, 1975; Tessier *et al.*, 1979) because of their strong bearing on the nature and characteristics of sediments and also the environment under which the sediments are being deposited (Jackson, 1967). In the present study, ammonium acetate extraction method of Gupta and Chen (1975) was used to extract the exchangeable fraction of the alkali and alkaline earth elements in the core. After washing a known amount of sediment with double distilled water, 1N ammonium acetate was added and then shaken for 90 minutes on a mechanical shaker. The exchangeable phase was separated by centrifugation and membrane filtering. The extract was then estimated for alkali and alkaline earth metals using Atomic Absorption Spectroscopy (AAS). Apart from this, the bulk sediment samples were digested with  $\text{HNO}_3 + \text{HClO}_4$  acid mixture and analysed for heavy metals like Fe, Mn, Cu, Zn and Ni to know their level variabilities non-silicate bound phases in the sediments. The analytical results were checked against standard rock and sediment samples and the results were in agreement with the certified values. Statistical software package SPSS version 16 was used for data processing and cluster analysis. The dataset used for the analysis comprises 27 variables including major and trace elements, LOI, sand, silt and clay percentages in the 9 subsamples of the core. Data standardization has been achieved by z-transformation using SPSS 16.0 software. For measuring the similarity between the variables, squared Euclidean distance was preferred as it accelerates the clustering process by amplifying the

**Table 2:** Equation used for calculating the statistical parameters (*After folk and Ward, 1957*).

Sl. No	Statistical Parameters	Formula
1	Mean	$\frac{\phi_{16} + \phi_{50} + \phi_{84}}{3}$
2	Standard deviation	$\sqrt{\frac{\phi_{84} - \phi_{16}}{4} + \frac{\phi_{95} - \phi_{5}}{6.6}}$
3	Skewness	$\frac{\phi_{16} + \phi_{84} - 2\phi_{50}}{2(\phi_{84} - \phi_{16})} + \frac{\phi_{5} + \phi_{95} - 2\phi_{50}}{2(\phi_{95} - \phi_{5})}$
4	Kurtosis	$\frac{\phi_{95} - \phi_{5}}{2.44(\phi_{75} - \phi_{25})}$

influence of outliers and larger dissimilarities, which can help differentiate distinct groups more effectively. The dendrogram was generated using Ward's method that provide a visual representation of the hierarchical structure and offers insights into the appropriate number of clusters based on how the groups were interlinked.

## Results

### Sediments

#### Lithology and Sediment Characteristics

The 30 m long borehole core used for the present study is composed essentially of two major lithological units, the top 14.7 m is a sand-dominant layer, which rests over a thick silty clay layer (Fig. 3). The inter-relationship between sand, silt and clay in the samples and their sediment facies is depicted in the ternary diagram of Picard (1971) (Fig. 4). Table 3 shows the sand, silt and clay contents of the borehole core along with organic carbon contents. The sand layer is dominated by coarse and medium sand. The content of sand showed a marginal deviation at 9-10.5 m depth

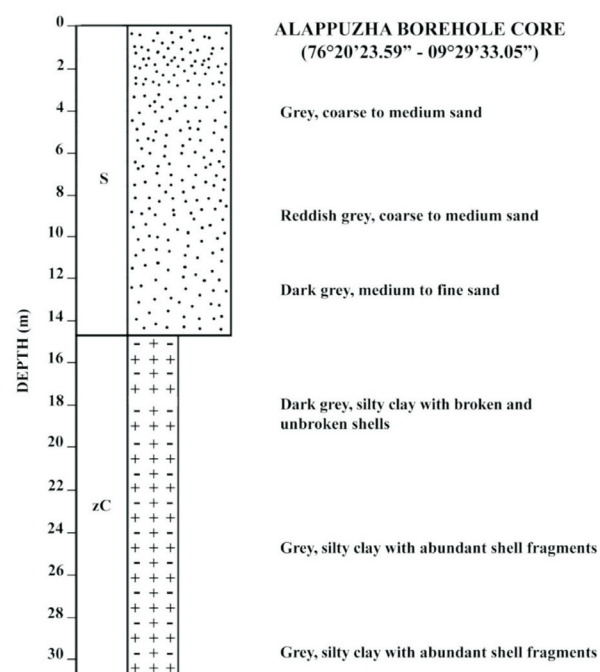


**Fig.3.** Lithology and characteristics of the sediments in Alappuzha borehole core. S: Sand; zC: Silty clay.

**Table 3:** Sand, silt, clay, mud (Silt + Clay) and organic carbon contents ( $C_{org}$ ), and classification (After Picard 1971) of the sediments obtained in the Alappuzha borehole core.

Sample depth (m)	Sand %	Silt %	Clay %	Mud %	C-org %	Sediment type (Picard, 1971)
1.0	95.59	3.63	0.78	4.41	0.32	Sand
4.5	97.93	0.55	1.52	2.07	0.48	Sand
6.0	95.69	0.92	3.39	4.31	0.24	Sand
10.5	97.6	1.28	1.12	2.40	0.20	Sand
12.0	86.92	3.03	10.05	13.08	0.44	Sand
13.5	88.46	7.82	3.72	11.54	0.40	Sand
15.0	4.23	26.69	69.08	95.77	19.95	Silty Clay
19.0	7.35	20.96	71.69	92.65	13.97	Silty Clay
25.0	19.94	28.63	51.43	80.06	7.98	Silty Clay
30.0	16.78	30.15	53.07	83.22	7.98	Silty Clay

$C_{org}$  Organic carbon; The values are in percentages

where the sands are slightly in the fine class. The underlying silty clay layer is dominated by medium and fine clay. The vertical variation of size spectral characteristics of the borehole core is depicted in Fig. 5. The mean size of the borehole sediments varies from  $1.42 \phi$  (medium sand) to  $9.0 \phi$  (clay). The sand-dominated samples are moderately well sorted ( $\sigma 0.68 \phi$ ) to very poorly sorted ( $\sigma 2.25 \phi$ ). The lower silty clay sediments are very poorly sorted ( $\sigma 1.86 \phi$  to  $3.11 \phi$ ). The samples obtained at 9 m and 10.5 m depths exhibit negative skewness (-0.10 & -0.11) indicating winnowing of finer particles from the size population by return wash on a beach environment (Blatt *et al.*, 1972). The kurtosis ( $K_g$ ) of the samples in general show platy (1.33) to leptokurtic (1.018) distribution (Table 4).

#### Heavy Minerals

The total heavy mineral (THM) contents vary widely in the borehole core from 1.49% to 10.51% with an average of 5.02% (Table 5). The upper part of the sand layer contains high concentration of THM (6.39 – 10.51%; average 8.45%) compared to its lower part (1.49 – 3.80%; average 3.53%). The sand content in the lower mud dominated layer records an average THM content of 5.22% (range 3.66 – 6.50%) (Table 5). The total light minerals (TLM) vary from 89.49% to 98.51% with an average of 94.97%.

**Table 4:** Statistical parameters of the Alappuzha borehole core

Sample depth (m)	Statistical parameters				
	Mean ( $\phi$ )	Standard deviation ( $\sigma$ )	Skewness (Sk)	Kurtosis (Kg)	
1.0	1.53	0.79	0.02	1.22	
2.0	1.63	0.80	0.06	1.18	
3.0	1.50	0.78	0.01	1.26	
4.5	1.42	0.68	-0.06	1.33	
6.0	1.83	0.89	0.07	0.99	
7.5	1.80	0.96	0.02	0.98	
9.0	2.23	0.96	-0.10	1.02	
10.5	2.25	0.92	-0.11	1.04	
12.0	1.63	1.14	0.08	0.89	
13.5	1.93	1.22	-0.20	0.83	
15	9.0	2.01	-0.66	1.04	
17	8.98	1.86	-0.57	0.83	
19	8.81	2.35	-0.66	1.10	
21	7.46	3.11	-0.44	0.81	
23	7.88	2.75	-0.45	0.86	
25	7.45	2.84	-0.31	0.66	
27	7.97	2.48	-0.24	0.81	
30	7.95	2.61	-0.26	0.88	

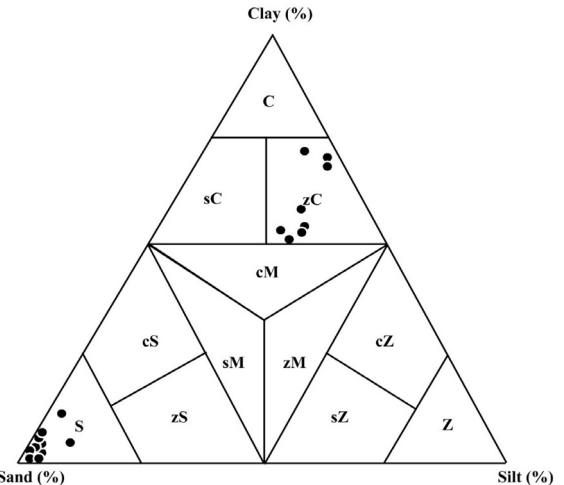


**Fig.4.** Sediment types (after Picard 1971) of the Alappuzha borehole core. S Sand, zS Silty sand, cS Clayey sand, sM Sandy mud, zM Silty mud, cM Clayey mud, sZ sandy silt, cZ Clayey silt, Z Silt, sC Sandy clay, zC Silty clay, C Clay

Opaque (32.33 – 67.63%; av. 56.33%) and sillimanite (30.43 – 64.68%; av. 40.63%) are the predominant minerals in the heavy mineral suite. Zircon is present in most of the samples in small amounts. Traces of garnet is also noticed at the surface of the sand dominated layer. The TLM is composed mainly of the mineral quartz with small quantities of broken/complete shells and feldspar grains.

#### Macro and Microfauna

The borehole sediments contain broken and complete shells of bivalves, gastropods and other calcareous skeletal parts. *Venus*,

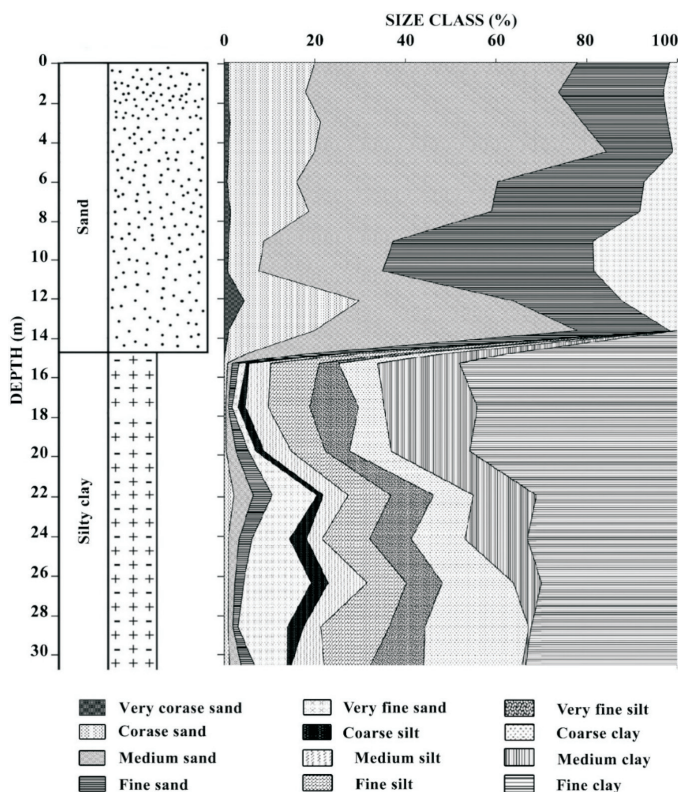


**Fig.5.** Size spectral image of the Alappuzha borehole core.

**Table 5:** Heavy mineral contents in the Alappuzha borehole core sediments. The total heavy minerals (THM) and total light minerals (TLM) values are expressed in weight percentage and others are in number percentage

Borehole Depth (m)	THM (Wt %)	TLM (Wt %)	Heavy Minerals (number %)									
			Opaque	Sillimanite	Zircon	Rutile	Monazite	Garnet	Inosilicate	Biotite	Sphene	Others
1.0	6.39	93.61	53.71	41.48	0.87	-	-	1.31	1.31	-	-	1.31
3.0	10.51	89.49	64.62	30.77	-	-	-	1.23	-	-	-	1.85
6.0	1.49	98.51	54.81	43.27	0.96	-	-	-	-	-	-	0.96
9.0	2.29	97.61	32.33	64.68	0.50	-	-	-	-	-	-	2.49
13.5	3.80	96.20	67.63	30.43	0.48	0.48	-	-	-	-	-	0.97
17.0	5.49	94.51	64.29	35.71	-	-	-	-	-	-	-	-
25.0	6.50	93.50	62.07	34.48	-	-	-	-	-	-	-	3.44
30.0	3.66	96.33	51.21	44.25	0.88	-	-	0.88	0.88	-	-	0.88

*Donax, Cardium and Anadara* are some of the bivalves identified in the core sediment. The microfauna identified (Fig. 6) include foraminifers *Ammonia*, *Bolivina*, *Elphidium* and *Virgulina*, besides a few sea urchin spines and juvenile forms of gastropods and bivalves. The list of microfauna along with preferred habitat of occurrence is furnished in Table 6.

### Geochemistry

#### Organic carbon ( $C_{org}$ )

The organic carbon ( $C_{org}$ ) content in the core varies from 0.20% to 19.95% with an average of 5.2% (Table 3). The highest  $C_{org}$

$C_{org}$  value was noticed for silty clay layer at the sand-clay interface (at a depth of 15 m). The upper sandy layer had an average  $C_{org}$  content of 0.35 % with a maximum value of 0.48% and minimum value of 0.2%. The silty clay layer shows markedly high content of organic carbon with an average of 12.47%.

#### Major and Trace Elements

Table 7 shows the content of major elements as oxides in the sediment samples along with loss on ignition (LOI) in percentages. The LOI correlates generally with the organic carbon content in the sediments because of their strong dependence; but the shells and moisture content in the sediments could also influence the LOI

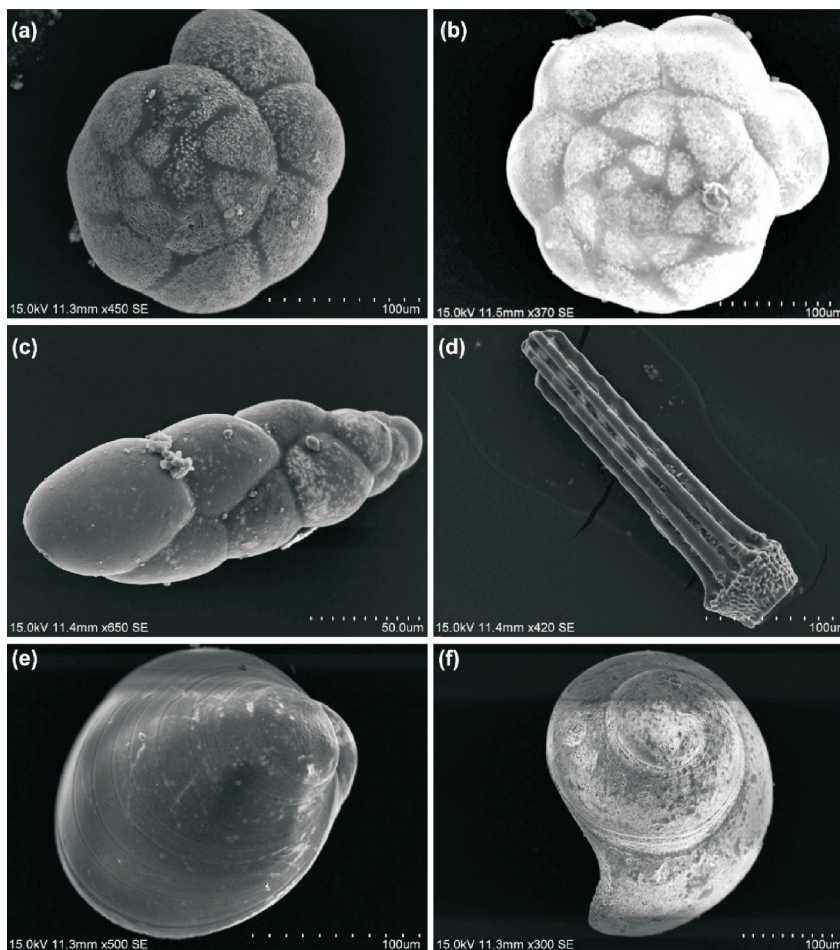


**Fig.6.** Microfauna recovered from the borehole: a & b) *Ammonia beccari* from a depth of 21 and 30 m in the borehole; c) *Virgulina* from 21 m; d) Echinoid (sea urchin) spine from 21 m; e) Bivalve veliger from 9 m; f) Gastropod veliger from 9 m.

**Table 6:** Microfauna found in the borehole and their respective habitats

Taxa	Habitat	Reference
1 <i>Ammonia</i>	Found mainly in shallow water, saline to brackish water environments	Murray (1973)
2 <i>Bolivina</i>	Deltaic and shallow marine environments	Obiosio (2013)
3 <i>Elphidium</i>	Brackish and shallow marine environments	Murray (1991)
4 <i>Virgulina</i>	Nearshore and shallow marine environments	Smith (1964)
5 Sea urchin spine	Shallow to deep marine, sandy to rocky bottom	Elmasry <i>et al.</i> (2013)
6 Gastropod veliger	Live in water column, marine environment	Fish and Fish (1977)
7 Bivalve veliger	Live in brackish water/nearshore environments	Hornell (1921)

values. The samples are dominated by  $\text{SiO}_2$  and it ranges from 53.1% to 98.83% (average of 77.01%). The  $\text{SiO}_2$  content is substantially higher in the upper sandy layer (average of 95.08%). The slightly lower value of  $\text{SiO}_2$  (88.9%) in the sample collected at a depth of 12 m, can be attributed to the comparatively higher content of finer sediments than the upper and lower parts of the sandy sediments. The  $\text{SiO}_2$  content is markedly lower in the silty clay layer (53.1 – 57.7%, an average of 54.44%). The content of  $\text{TiO}_2$  also shows contrasting values between the upper sandy layer (0.71%) and the lower silty clay layer (1.09%). At the depth of 12 m, the value of  $\text{TiO}_2$  is the highest (1.29%). The  $\text{Al}_2\text{O}_3$  content is substantially lower (1.39% on average) in the sandy upper layer while the lower muddy layer is about 10 times more enriched (an average of 14.46%). The  $\text{Fe}_2\text{O}_3$ ,  $\text{CaO}$ ,  $\text{MgO}$ ,  $\text{Na}_2\text{O}$ ,  $\text{K}_2\text{O}$ , and  $\text{P}_2\text{O}_5$  contents also show a similar trend with substantially lower values in

the sandy layer and higher values in the muddy layer. However, a small increase is noticed in the middle level of the core at 12m below ground level as the layer is generally with finer sands.

As seen from Table 8, the content of  $\text{SiO}_2$  shows a negative correlation with all the other oxides, whereas  $\text{Al}_2\text{O}_3$  and  $\text{Fe}_2\text{O}_3$ , show a strong positive correlation with  $\text{CaO}$ ,  $\text{Na}_2\text{O}$ ,  $\text{K}_2\text{O}$ , and  $\text{P}_2\text{O}_5$ , indicating their co-existence in the muddy sediments in the lower part of the core.  $\text{MnO}$  deviates slightly from the other major elements although it shows a significant positive relation with  $\text{Fe}_2\text{O}_3$ .

Among the trace elements (Table 9), V, Cr, Rb, Sr, Y, Zr and La are recorded in all samples. Ni, Zn and Ba were below detection limits in the sand dominated samples and Cu is present in all the silty clay samples and also in two sand dominated samples. With exception of Zr, all the other elements are enriched in the silty clay sediments (Table 10), whereas Zr shows an enrichment in the sandy layer, possibly due to the presence of the mineral zircon [a zirconium silicate mineral ( $\text{ZrSiO}_4$ )] in the sediment samples (Table 5). The inter relationship between the trace elements shows a significant negative correlation of Zr with the other elements, whereas all the other elements show a strong positive correlation among each other (Table 10). The relationship is shown in the dendrogram (Fig. 7), indicating that  $\text{Al}_2\text{O}_3$ ,  $\text{Fe}_2\text{O}_3$ ,  $\text{MgO}$ ,  $\text{Na}_2\text{O}$ ,  $\text{K}_2\text{O}$ , and  $\text{P}_2\text{O}_5$  and the trace elements Ni, Cr, Ba, V and La are linked to the finer clastics. This cluster is linked to Ga, Y and Cu, and also C-org,  $\text{MnO}$ ,  $\text{CaO}$ , Sr and  $\text{TiO}_2$  at fairly significant levels. The content of sand,  $\text{SiO}_2$  and Zr deviates and form a separate cluster (Fig. 7; Table 10). All other elements are associated at different levels in the silt and clay dominated sediments.

#### Exchangeable Cations- Extraction Studies

The content of the exchangeable cations Ca, Mg, Na and K

**Table 7:** XRF data showing the content major elements in the borehole core sediments. Except  $\text{SiO}_2/\text{Al}_2\text{O}_3$ , all others are in percentages

Depth	$\text{SiO}_2$ (%)	$\text{TiO}_2$	$\text{Al}_2\text{O}_3$	$\text{MnO}$	$\text{Fe}_2\text{O}_3$	$\text{CaO}$	$\text{MgO}$	$\text{Na}_2\text{O}$	$\text{K}_2\text{O}$	$\text{P}_2\text{O}_5$	LOI	Total	$\text{SiO}_2/\text{Al}_2\text{O}_3$
1	94.65	0.96	1.62	0	0.56	0.23	0.05	0.19	0.03	0.05	1.61	99.93	58.4
4.5	96.74	0.87	0.8	0	0.36	0.18	0.01	0.15	0	0.03	0.79	99.93	120.9
6	98.83	0.28	0.33	0	0.02	0.14	0	0.11	0.01	0.02	0.22	99.97	299.4
10.5	96.31	0.73	1.09	0	0.16	0.8	0.08	0.15	0.14	0.03	0.41	99.91	88.3
12	88.89	1.29	3.13	0	1.18	1.93	0.8	0.32	0.33	0.07	1.92	99.88	28.3
15	53.1	1.07	14.49	0.7	8.39	1.98	3.84	1.2	1.86	0.2	13.73	99.91	3.6
19	53.13	1.09	14.7	0.7	8.98	1.77	3.8	1.12	1.87	0.2	13.15	99.89	3.6
25	57.7	1.12	14.52	0.05	7.24	4.2	3.5	1.56	1.94	0.22	7.83	99.87	3.9
30	53.81	1.07	14.14	0.05	8.14	4.5	3.77	1.42	1.87	0.25	10.86	99.88	3.8

**Table 8:** Correlation matrix of major elements in the core sediments

	Sand	Silt	Clay	$\text{SiO}_2$	$\text{TiO}_2$	$\text{Al}_2\text{O}_3$	$\text{MnO}$	$\text{Fe}_2\text{O}_3$	$\text{CaO}$	$\text{MgO}$	$\text{Na}_2\text{O}$	$\text{K}_2\text{O}$	$\text{P}_2\text{O}_5$	LOI
Sand	1													
Silt	-0.961**	1												
Clay	-0.993**	0.923**	1											
$\text{SiO}_2$	0.995**	0.970**	-0.983**	1										
$\text{TiO}_2$	-0.500	0.498	0.490	-0.558	1									
$\text{Al}_2\text{O}_3$	-0.993**	0.975**	0.978**	-0.997**	0.551	1								
$\text{MnO}$	-0.723*	0.523	0.790	-0.678	0.291	-0.658	1							
$\text{Fe}_2\text{O}_3$	-0.997**	0.958**	0.990**	-0.997**	0.522	0.993**	0.711*	1						
$\text{CaO}$	-0.744*	0.860**	0.678	-0.789	0.572	0.800**	0.109	0.751*	1					
$\text{MgO}$	-0.995**	0.970**	0.983**	-0.998**	0.543	0.997**	0.672*	0.995**	0.798**	1				
$\text{Na}_2\text{O}$	-0.954**	0.990**	0.917**	-0.966**	0.533	0.997**	0.492	0.953**	0.888**	0.968**	1			
$\text{K}_2\text{O}$	-0.990**	0.978**	0.973**	-0.994**	0.527	0.998**	0.636	0.989**	0.818**	0.996**	0.982**	1		
$\text{P}_2\text{O}_5$	-0.966**	0.987**	0.936**	-0.983**	0.573	0.984**	0.539	0.973**	0.873**	0.982**	0.986**	0.984**	1	
LOI	-0.979**	0.907**	0.986**	-0.971**	0.507	0.958**	0.813**	0.980**	0.637	0.966**	0.883**	0.947	0.923**	1

\* Significant at the 0.05 level (2-tailed); \*\* Significant at the 0.01 level (2-tailed)

**Table 9:** X-ray fluorescence measurements of trace elements in the core sediments (in ppm).

Depth	V	Cr	Ni	Cu	Zn	Ga	Rb	Sr	Y	Zr	Ba	La
1	106	41	0	8	0	0	14	34	2	609	0	18
4.5	94	37	0	0	0	0	12	33	2	635	0	9
6	73	34	0	14	0	0	12	34	1	197	0	9
10.5	90	48	0	0	0	0	15	60	1	764	0	9
12	116	63	2	0	0	0	21	79	3	949	65	14
15	143	183	76	15	52	10	62	100	10	118	270	27
19	144	191	84	20	57	15	72	120	22	194	271	36
25	136	161	68	12	34	9	66	164	10	343	359	28
30	138	175	87	19	54	17	75	195	21	299	229	24

shows an increasing trend towards the bottom of the core (Table 11). The upper sand layer shows an average of 1,266 ppm of Ca, 348 ppm of Mg, 33 ppm of Na and 8 ppm of K. The average concentration of the exchangeable cations is about 5 times higher in the silty clay sediments with 6440 ppm of Ca, 2697 ppm of Mg, 425 ppm of Na and 119 ppm of K. The upper half of the sand layer shows comparatively lower level of cations in its lower half.

### Heavy Metals in the Non-Silicate Phase

The downcore variations of heavy metals (Table 12) such as Fe, Mn, Cu, Zn and Ni in the  $\text{HNO}_3 + \text{HClO}_4$  acid digested samples (six samples from the upper sand layer and four samples from the lower silty clay) were examined to understand its level variabilities in the non-silicate phase of sediment samples. The concentration of Fe in the sediments varies from 0.11% to 6.89% with an average of 2.14%, and is generally related to the grain size characteristics of the sediments. The sandy layer contains lower concentration of Fe, varying from 0.11% to 0.36% with an average of 0.22%, whereas the silty clay at the lower half of the core exhibits markedly higher concentration of Fe with a minimum of 3.89% and maximum of 6.89% (average of 5.02%). As seen from the Table 13, it is clear that Fe shows strong positive correlation with clay ( $r^2 = 0.982$ ) and silt ( $r^2 = 0.881$ ) as well as organic carbon ( $r^2 = 0.896$ ) contents. The concentration of Mn shows an average of 172 ppm (BDL to 505 ppm). Like the distribution of Fe, the content of Mn is comparatively low in sand dominant sediments (average of 16.3 ppm) than in the silty clay sediments (average of 405 ppm).

The maximum, minimum and average concentration of Cu in the bulk sediments of the core (Table 12) are 25 ppm, 60 ppm and 49 ppm respectively. Unlike Fe and Mn, the content of Cu does not show any specific granulometric dependence. The content of Zinc

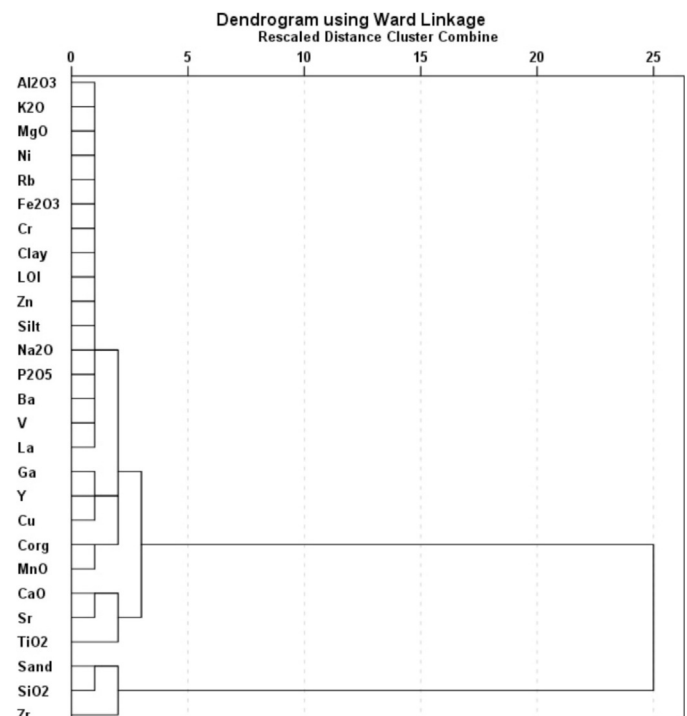


Fig.7. Dendrogram showing the relationship between major and trace elements along with sand, silt, clay fractions of the cored sediments.

varies from 30 to 195 ppm (av. 72 ppm). The upper sand layer contains lower concentration of Zn (BDL to 52 with an average of 34 ppm) compared to the lower silty sediments (80 ppm to 195 ppm, average 129 ppm). The heavy metals examined in this study shows a negative correlation with sand percentage in the sampled sediments (Table 13).

### Discussion

Coastal areas are the most diverse and dynamic environments on the earth influenced by many geological, oceanographic, biological and human activities. The interplay between these processes is responsible for shaping a unique array of landforms in the coastal environment. The study and interpretation of various processes operating the coast are of much importance in understanding the coastal environments and their evolutionary history. Among the different approaches in the study of the coastal

**Table 10:** Correlation matrix of trace elements from the core sediments

	Sand	Silt	Clay	V	Cr	Ni	Cu	Zn	Ga	Rb	Sr	Y	Zr	Ba
Sand	1													
Silt	-0.961**	1												
Clay	-0.993**	0.923**	1											
V	-0.916**	0.885**	0.908**	1										
Cr	-0.996**	0.955**	0.991**	0.930**	1									
Ni	-0.988**	0.966**	0.975**	0.895**	0.990**	1								
Cu	-0.780*	0.743*	0.778*	0.574	0.759*	0.808**	1							
Zn	-0.980**	0.930**	0.979**	0.884**	0.983**	0.990**	0.821**	1						
Ga	-0.935**	0.915**	0.922**	0.847**	0.948**	0.976**	0.825**	0.974**	1					
Rb	-0.982**	0.970**	0.964**	0.912**	0.988**	0.994**	0.777*	0.972**	0.970**	1				
Sr	-0.827**	0.906**	0.775*	0.797*	0.847**	0.868**	0.600	0.807**	0.874**	0.908**	1			
Y	-0.871**	0.823**	0.871**	0.818**	0.895**	0.921**	0.793*	0.928**	0.977**	0.922**	0.824**	1		
Zr	0.700*	-0.651	-0.705*	-0.400	-0.653	-0.702*	-0.900**	-0.720*	-0.663	-0.641	-0.398	-0.580	1	
Ba	-0.956**	0.950**	0.937**	0.894**	0.949**	0.932**	0.673*	0.887**	0.849**	0.949**	0.854**	0.776*	-0.603	1

\* Significant at 0.01 level (2-tailed) \*\* Significant at 0.05 level (2-tailed)

**Table 11.** Concentration of exchangeable metals in the core sediments

Sl. No.	Sample Depth (m)	Ca	Mg (ppm)	Na	K
1	1.0	320	49	16	5
2	4.5	640	49	14	3
3	6.0	160	49	12	3
4	10.5	1520	194	26	6
5	12.0	2320	1118	60	14
6	13.5	2640	632	70	19
7	15.0	8880	1604	418	136
8	19.0	6080	2381	390	133
9	25.0	4800	3013	518	127
10	30.0	6000	3791	374	83

**Table 12:** Concentration of heavy metals in the non-silicate phase of the Alappuzha borehole core sediments (BDL: below detection limit).

Sl. No.	Sample Depth (m)	Fe (%)	Mn	Cu	Zn	Ni
1	1.0	0.16	BDL	40	32	BDL
2	4.5	0.22	28	55	45	BDL
3	6.0	0.13	BDL	57	30	BDL
4	10.5	0.11	BDL	60	45	BDL
5	12.0	0.36	40	47	52	BDL
6	13.5	0.34	30	25	BDL	BDL
7	15.0	4.77	445	55	137	63
8	19.0	6.89	505	57	195	75
9	25.0	3.89	298	45	80	45
10	30.0	4.52	373	50	102	48

**Table 13:** Correlation matrix of heavy metals in the non-silicate phase as well as sand, silt, clay and C-org percentages in the Alappuzha borehole core sediments

Variable	C <sub>org</sub>	Sand	Silt	Clay	Cu	Fe	Mn	Ni	Zn
C <sub>org</sub>	1.000								
Sand	-0.918**	1.000							
Silt	0.815**	-0.961**	1.000						
Clay	0.940**	-0.993**	0.923**	1.000					
Cu	0.174	-0.016	-0.133	0.77	1.000				
Fe	0.889**	-0.967**	0.881**	0.981**	0.110	1.000			
Mn	0.932**	-0.983**	0.904**	0.994**	0.113	0.990**	1.000		
Ni	0.934**	-0.979**	0.894**	0.992**	0.122	0.993**	0.995**	1.000	
Zn	0.879**	-0.869**	0.711*	0.915**	0.263	0.951**	0.940**	0.943**	1.000

\*\* 0.01 Correlation is significant at the 0.01 level 2-tailed \* 0.05 Correlation is significant at the 0.001 level 2-tailed

environments, the textural and geochemical investigations receive considerable importance as these studies can throw light on the different coastal processes and the depositional environments.

The ternary diagram (Fig. 4, 8) showing the relative sand, silt and clay percentages in the samples reveals that the plots are segregated in two distinct clusters, one close to the clay-dominated area and the other in the sand dominated area. The sedimentary succession (Fig. 8) indicates the existence of two distinct energy regimes existed during the deposition of sediments in the borehole site. There are four different sectors in the ternary diagram indicating different energy fields from I to IV of Pejrup (1988), representing the quietest to most violent energy environments. In the present ternary plot (Fig. 8) the samples are clustered mainly in the sectors II and III indicating a moderate energy regime (*i.e.*, not very low or not very high) that prevailed during the deposition of the muddy (silt + clay admixed) sediments (Fig. 3). However, a few samples deviate from this general trend probably because of high energy depositional conditions at the time of deposition of the upper succession.

Various parameters such as grain size distribution, the shape of cumulative curves, frequency curves, and various other calculated parameters, have been used as environmental indicators. Passeggi (1957, 1964) suggested that a diagram showing Median (M) of the grain size population curve against its 1 percentile (C), *i.e.*, CM diagram, will be very useful for the study of the kind of transportation of sediments in the given environment. In general, there are three main modes of transportation of sediments rolling, suspension and saltation.

The maximum grain size of sediment that may come in suspension will be less than 0.1 mm (Lane, 1938). However, the values vary significantly in different environments and depend upon the hydrodynamic conditions at the time of sedimentation. In the present study, about 50% of the samples fall on the PQ segment

of the C/M diagram (Fig. 9) indicating transport of the sand fraction by suspension and rolling. However, the samples from the muddy layer form a separate cluster as the particles are transported generally as suspension. The lower silty clay sediments in the borehole could have been accumulated on a low-energy marine to brackish environment such as a lagoon or embayment, as suggested by the foraminifera species in the faunal assemblage (Fig. 6, Table 6). This is further supported by the strong positive correlation of organic carbon with silt (0.817) and clay (0.943) contents as the finer particles and organic matter are deposited together in low energy environments. Furthermore, it is axiomatic that the finer particles are very efficient in trapping organic matter derived from

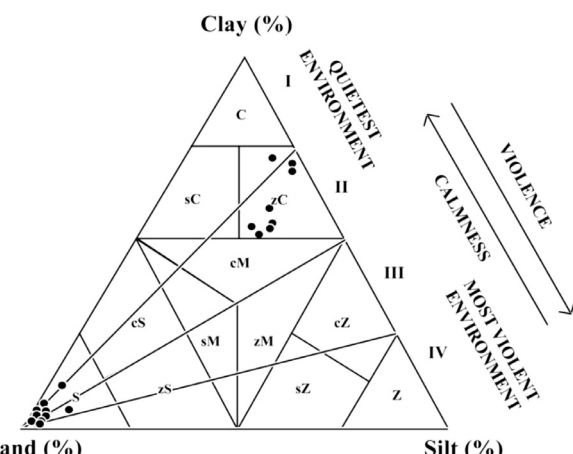


**Fig. 8.** Ternary diagram showing sediment types in relation to depositional environments (*after* Picard 1971; Pejrup, 1988). I to IV indicates the different energy regimes from calm (I) to most violent (IV). S Sand, sZ Silty sand, cS Clayey sand, sM Sandy mud, zM Silty mud, cM Clayey mud, sZ sandy silt, cZ Clayey silt, Z Silt, sC Sandy clay, zC Silty clay, C Clay.

authigenic and alloogenetic sources (Hackanson and Jansson, 1983; Padmalal and Seralathan, 1995). On the other hand, the coarse-skewed sandy layer show comparatively higher energy depositional conditions, possibly related to the development of the coastal barrier in the study area as described earlier by Padmalal *et al.* (2014a).

The geochemistry of sediments is the outcome of many factors. The source rock characteristics, degree of chemical weathering in the source area, sediment sorting, nature and characteristics of the depositional environments, organic and inorganic carbon fluxes etc., are some of the factors that could determine the net chemical composition of the sediments (Bjørlykke, 2010). The content of  $\text{Al}_2\text{O}_3$  shows a drastic difference in the two lithounits of the Alappuzha borehole core. In the clay dominated layer, the  $\text{Al}_2\text{O}_3$  content exhibits 10 times enrichment compared to that in the overlying sand layer. This might be due to the reduced supply of aluminosilicates like feldspars and clay minerals in the sand dominated layer. The size and density-based sorting which was prevalent during the formative phases of the upper sand layer could attribute the foresaid changes in the geochemical characteristics of sediments. As seen from Table 8, most of the major elements are negatively correlated with  $\text{SiO}_2$ , suggesting the role of quartzose sand in the bulk sediments in determining the concentration variabilities of elements (Padmalal and Seralathan, 1995; Padmalal *et al.*, 1997). The  $\text{SiO}_2/\text{Al}_2\text{O}_3$  ratio show a decreasing trend downcore, indicating deposition of finer clastics rich in aluminosilicate clay minerals which can enhance the  $\text{Al}_2\text{O}_3$  contents relative to the  $\text{SiO}_2$  contents. The dominant quartz sand in the upper half of the core is essentially brought by the longshore drift of sediments and is rather well sorted compared to the silty clay dominated lower half of the core. Marine clays are dominated generally by montmorillonite clay mineral which contains alkali elements like Na and K and alkali earth elements like Ca and Mg. The content of exchangeable cations like Na, K, Ca and Mg in the sediments and sedimentary formations could determine the quality of groundwater in the aquifer systems. In the Alappuzha core, the sand dominated upper layer contains comparatively lower level of alkali and alkaline earth elements than the lower silty clay layer. This is generally because the organic matter rich clay dominated lagoonal sediments undergo diagenetic remobilization of the exchangeable elements and these elements will later be deposited in the pore fluids of the silty clay sediments first and then move towards the sand column in the top during sediment compaction process. The strong positive correlation of Fe with silt, clay and organic matter indicates that a conducive environment is existing in the sediments favorable for early diagenetic remobilization of elements in the system. Further, the correlation also reiterates the fact that a substantial part of Fe is associated with finer particles that are known for trapping organic matter derived from alloogenetic and authigenic sources (Hakanson and Jansson, 1983). The higher concentration of organic matter with silt and clay substantiates this view. The Fe exhibits strong positive correlation with Mn as Fe and Mn precipitate together in aquatic environments under oxidizing conditions (Padmalal and Seralathan, 1995). The granulometric and mineralogical composition will have a strong bearing on the distribution of Mn in the borehole sediments. As the upper sand layer is rich in quartzose sand, the layer cannot hold much Mn contents within the sediments. On the other hand, the clay minerals that are rich in silty clay can carry substantially high content of Mn because of higher surface area of the particles and its

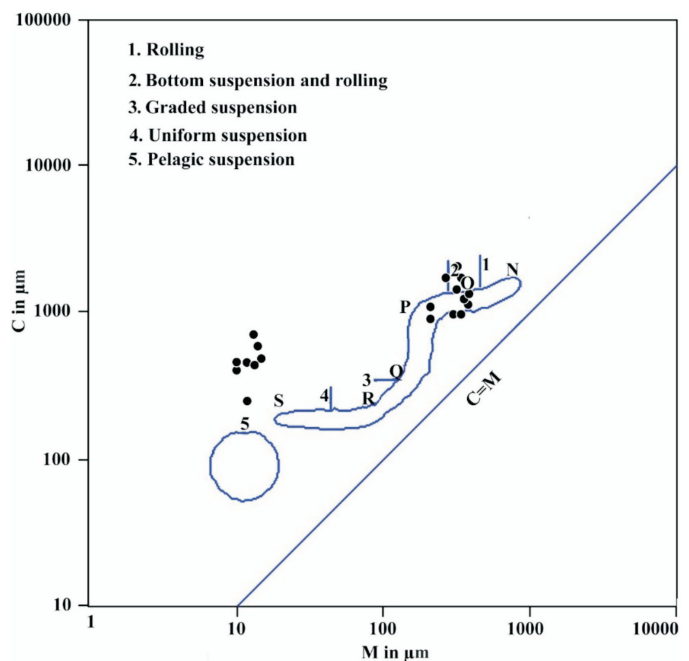


**Fig.9.** C/M diagram showing modes of transportation of the cored sediments (after Passeggi, 1964; Dinesh, 2009). The letter N, O, P, Q, R, and S are the limiting points within which the particulates will be moved in different ways—Rolling (1), Bottom suspension and rolling (2), graded suspension (3), Uniform suspension (4) and Pelagic suspension (5).

cation exchange capability. Further, the region from which the sediment core is lifted was a part of coastal nearshore environment which was later turned into a lagoon. Therefore, the saline water rich in Ca, Mg, Na and K during sedimentation will also be entrapped in the silty clays. The combination of these two processes might be the reason for the observed hike in alkali and alkaline earth elements in the exchangeable fractions. The occurrence of high fluoride content in the groundwaters of Alappuzha region (Raj and Shaji, 2017) further support the marine water entrapment during the formation of coastal landforms at Alappuzha.

Previous studies of Padmalal *et al.* (2014a, 2022) revealed that during Pre-Holocene, the Vembanad Lagoon was an embayment. The northward growth of the barrier beaches through accumulation of sediments transported by the longshore drift is responsible for the transformation of the embayment into Vembanad Lagoon (Padmalal *et al.*, 2014a; Maya *et al.*, 2022). The southern part of Vembanad Lagoon is much wider than the northern part, and coincides with the deepest subsiding part of the South Kerala Sedimentary Basin (SKSB) which is the landward extension of the subsiding Kerala Konkan Basin (Nair *et al.*, 2006). The latest subsidence in the area might have taken place in the late Holocene (Maya *et al.*, 2022), which together with the barrier spit development across the embayment might have responsible for the northerly diversion of the Achenkovil-Pamba-Manimala River systems and their ultimate linkages with the southern end of Vembanad Lagoon (Padmalal *et al.*, 2014a; Maya *et al.*, 2022). The abundant supply of sand transported by the longshore current would have favoured development of barriers and islands in the coastal area, a process also reported elsewhere (Carter *et al.*, 1989; Vaz *et al.*, 2002). The higher percent of sillimanite in the heavy mineral residue of the present study is consistent with the net northerly drift of sediments. The mineral sillimanite is an essential mineral in the khondalite which occurs in the hinterlands of the Trivandrum block

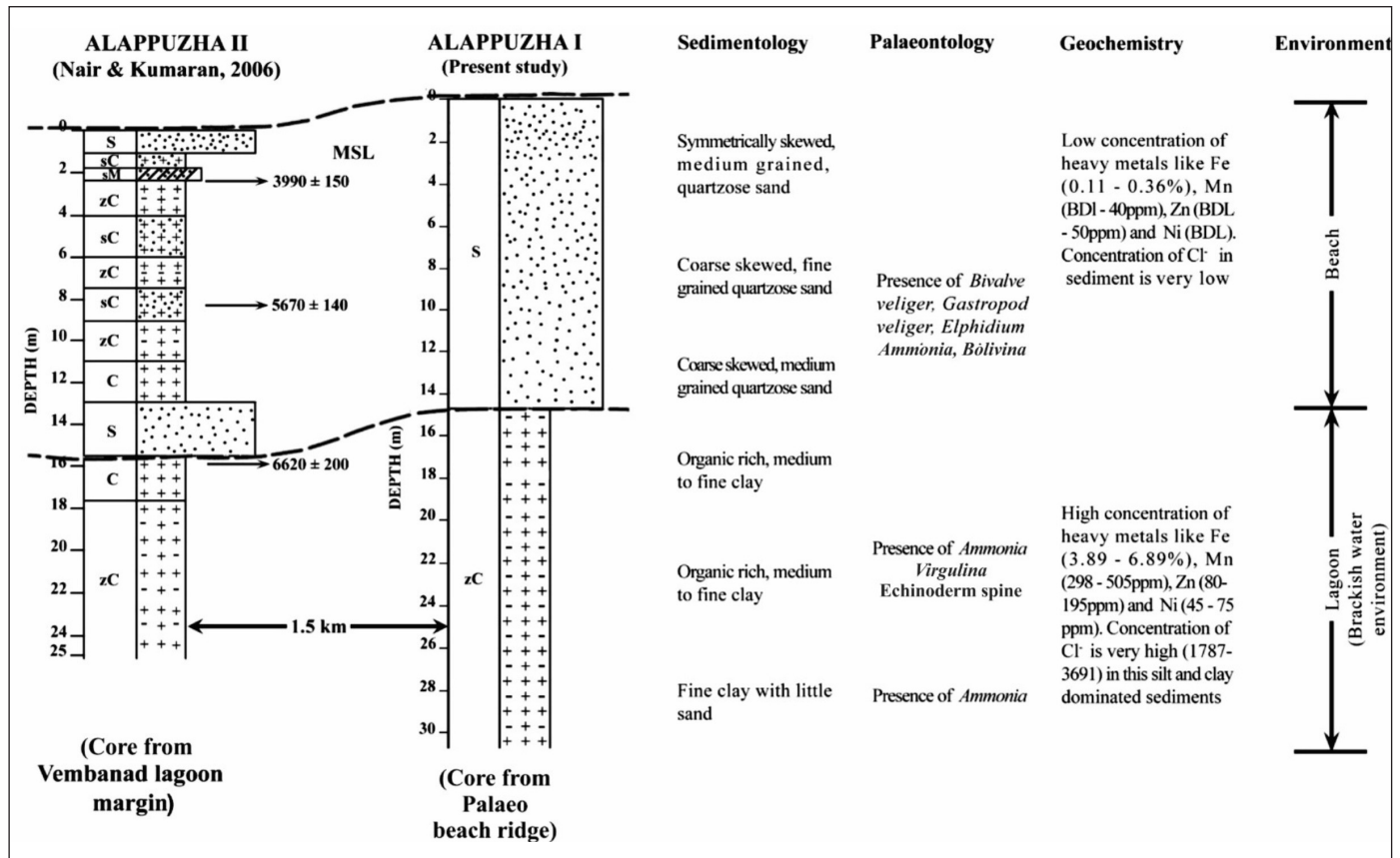


**Fig.10.** Correlation of the studied borehole core with that of a dated core of Nair and Kumaran (2006) retrieved from lagoon margin deposits.

in the southern side of the Achenkovil-Thenmala shear zone (Shimizu *et al.*, 2009; Praharaj *et al.*, 2021). The quantity and quality of heavy minerals including the sillimanites have been reported in many previous studies (Padmalal *et al.*, 2014b).

The bottom silty clay with shallow marine to brackish water forams and bivalves like *Venus* is indicative of lagoonal- nearshore environment. The comparison of the sediments of the present core with those of the Alappuzha II and Kalarkad cores described by Nair and Kumaran (2006) and Nair *et al.* (2006) reveals that the sand deposition in the cored area has begun in the Early-Middle Holocene (Fig. 10). The signatures of microfossil assemblages observed in the borehole cores indicated a shallow depositional regime, as indicated by foraminiferal taxa like *Ammonia*, *Bolivina* and *Virgulina*. In short, the study of the present core supports the fact that Vembanad Lagoon has been developed from the growth of a barrier spit across an embayment in the Early Holocene.

## Conclusions

Coastal environment is one of the most dynamic regions of the world which is undergoing profound changes consequent to rapid economic developments over the past few decades. The Kerala state in the southwest India has a long coastline and a considerable part of which is undergoing severe coastal erosion. A better understanding of how the coast has been evolved over the years is mandatory for future planning and developments. Therefore, a multi proxy study has been carried out in the present study using a 30m long borehole core retrieved from the coastal lowlands of Alappuzha district in the southwestern India to unravel

the nature and characteristics of the sediment build up in the area. Lithologically, the borehole core is composed of two units – the upper sand dominant layer and the lower silty clay layer with occasional presence of faunal remains of marine/brackish water affinity. The major element geochemistry of the core sediments shows a decreasing trend of SiO<sub>2</sub>/Al<sub>2</sub>O<sub>3</sub> ratio indicating enhanced supply of clay minerals from the hinterlands during the deposition of the lower lagoonal clays. The lagoonal clays account for high contents of alkali and alkaline earth elements in its non-silicate phase, presumably derived from the early diagenesis of the silty clays. The abundant occurrence of sillimanite in the heavy mineral crop of the borehole core indicates contribution of sediments from the khondalite dominated hinterlands of the Trivandrum Block in the southern side of the borehole site. Sillimanite is a typical lighter heavy mineral that can move along with the comparatively coarser quartz grains in the light mineral category during the northerly drift of sediments by the longshore currents. The mega and microfaunal assemblage together with the sedimentological and geochemical characteristics provide ample evidence of the evolution of the area from a shallow marine embayed environment to a barrier beach (shoreface) environment.

## Authors' Contributions

**AP:** Writing-Original Draft, Investigation, Conceptualization, Formal analysis. **PD:** Investigation, Conceptualization, Reviewing and Editing, Supervision. **VSM:** Investigation, Data Curation, Formal Analysis, Draft Figures. **DM:** Supervision.

## Conflict of Interest

The authors declare that there are no conflicts of interest.

## Acknowledgements

The authors thank the Centre for water resource development and management (CWRDM), Kozhikode and the National Centre

for Earth Science Studies, Thiruvananthapuram for chemical and sedimentological analysis. AP is indebted to Dr. P.S. Harikumar, Principal Scientist (Rtd.) for his guidance and support while carrying out sample preparation and analysis. Dr, Ratheesh Kumar, formerly with NCESS for identification of SEM images of the microfaunal remains. DP thanks the Director, NCESS for facilities and support. We are thankful to the reviewers who have given critical and thoughtful suggestions.

## References

- Anooja, S., Padmalal, D., Maya, K., Mohan, S. V. and Baburaj, B. (2013). Heavy mineral contents and provenance of Late Quaternary sediments of southern Kerala, Southwest India. *Indian Jour. Geo-Mar. Sci.*, v.42(6), pp. 749-757.
- Bagul, P. P., Kamble, P. B., Parab, O. and Herlekar, M.A. (2025). Seasonal Variations in Textural Characteristics and Sedimentary Environments of the Gaonkhadi Beach Sediments, Ratnagiri District, West Coast of India. *Jour. Geosci. Res.*, v.10(1), pp. 62-74.
- Bhatnagar, A., Shukla, A.D., Ngangom, M., Thakkar, M.G. and Chauhan, G. (2025). Temporal Changes in Land-Sea Configuration Inferred from Post-Glacial Sedimentation Pattern in the Western Great Rann of Kachchh, India. *Jour. Geosci. Res.*, v.10(1), pp. 1-6.
- Bjorlykke, K. (2010). Petroleum geoscience: From sedimentary environments to rock physics. Springer, Berlin. <https://doi.org/10.1007/978-3-642-34132-8>
- Blatt, H., Middleton, G.V. and Murray, R.C. (1972). Origin of Sedimentary rocks. Prentice Hall, New Jersey.
- Carter, L. (1974). An evaluation of the provenance of terrigenous sediments from offshore Vancouver Island. *Canad. Jour. Earth Sci.*, v.11, pp.664–677. <https://doi.org/10.1139/e74-064>
- Carter, R. W. G., Forbes, D. L., Jennings, S. C., Orford, J. D., Shaw, J. and Taylor, R. B. (1989). Barrier and lagoon coast evolution under differing relative sea-level regimes: examples from Ireland and Nova Scotia. *Mar. Geol.*, v.88, pp.221–242. [https://doi.org/10.1016/0025-3227\(89\)90099-6](https://doi.org/10.1016/0025-3227(89)90099-6)
- Centre for Earth Science Studies (1984). Resource atlas of Kerala. Centre for Earth Science Studies, Trivandrum.
- Chakraborty, J., Palit, K. and Das, S. (2022). Metagenomic approaches to study the culture-independent bacterial diversity of a polluted environment—a case study on north-eastern coast of Bay of Bengal, India. In: S. Das and H.R. Dash (Eds.), *Microbial Biodegradation and Bioremediation*, Elsevier, pp.81–107. <https://doi.org/10.1016/B978-0-323-85455-9.00014-X>
- Cherian, P. J. (2012). Pattanam archaeological site: Evidence of maritime exchanges. *Tamil Civil.*, v.12, pp.22-31.
- Cui, Z., Schulz-Bull, D. E., Hou, Y., Xia, Z. and Wanek, J. J. (2016). Geochemical characteristics and provenance of Holocene sediments (core STAT22) in the Beibu Gulf, South China Sea. *Jour. Coast. Res.*, v.32, pp.1105-1115.
- Das, P., Padmalal, D., Kumaran, K.P.N., Limaye, R.B., Mohan, S.V., Banerji, U.S. and Bhushan, R. (2024). Tracing the Late Quaternary coastal evolution of Central Kerala, India, around the lost ancient port Muziris using multi-proxy study of the sedimentary archives. *Quarter. Sci. Advanc.*, v.14, pp.100197.
- Dinesh, A.C. (2009). GSTAT-A software for grain size statistical analyses, CM Diagrams and Sediment Trend Maps Abstract Volume. International Seminar on Prospects of Marine sediments as Resource Base for the Man Kind (Abstract). Visakhapatnam.
- Danovaro, R. and Boero, F. (2019). Italian seas. In: C. Sheppard (Ed.), *An environmental evaluation*, Elsevier Ltd., pp. 283–306. <https://doi.org/10.1016/B978-0-12-805068-2.00060-7>
- Fish, J. D. and Fish, S. (1977). The veliger larva of *Hydrobia ulvae* with observations on the veliger of *Littorina littorea* (Mollusca: Prosobranchia). *Jour. Zool.*, v.182(4), pp.495-503.
- Folk, R.L. and Ward, W.C. (1957). Brazos River bar: a study in the significance of grain size parameters. *Jour. Sediment. Res.*, v.27, pp.3–26. <https://doi.org/10.1306/74D70646-2B21-11D7-8648000102C1865D>
- Gupta, S.K. and Chen, K.Y. (1975). Partitioning of trace metals in selective chemical fractions of nearshore sediments. *Environment. Letter.*, v.10, pp.129–158. <https://doi.org/10.1080/00139307509435816>
- Hanamond, P.T., Gawali, P.B., Lakshmi, B.V., Babu, J.M. and Deendayalan, K. (2017). Sediment texture and geochemistry of beaches between Redi-Vengurla, Sindhudurg, West Coast of India. *Jour. Coast. Res.*, v.33, pp.1135–1147. <https://doi.org/10.2112/JCOASTRES-D-15-00194.1>
- Håkanson, L. and Jansson, M. (1983). *Principles of lake sedimentology*. Springer.
- Hornell, J. (1923) The Common Molluscs of South India. *Nature*, v.111, pp.12. <https://doi.org/10.1038/111012d0>
- Jackson, M.L., Whittig, L.D. and Pennington, R.P. (1950). Segregation procedure for the mineralogical analysis of soils. *Proceed. Soil Sci. Soc. Am.*, v.14, pp.77–81.
- Jackson, M.L. (1967). *Soil Chemical Analysis*. Prentice-Hall of India, New Delhi.
- Joseph, A.M. and Gandhi, M.S. (2025) Spatial Distribution Analysis of Seasonal Variation in Salinity Stratification at Vembanad Estuary, Kerala, India. *Jour. Geosci. Res.*, v.10(1), pp. 36-43.
- KSLUB (1995). Land resources of Kerala State. Kerala State Land Use Board, Thiruvananthapuram.
- Kumar, R., Chatterjee, S., Kumar, R. and Deshmukh, B. (2023). Characteristics of Tidal Zone in Kalubhar Island, Gulf of Kachchh, Gujarat and Its Geomorphological Implications. *Jour. Geosci. Res.*, v.8(1), pp. 58-62.
- Lane, E.W. (1938). Notes on the formation of sand. *Eos. Transact. Am. Geophys. Union*, v.19, pp.505–508. <https://doi.org/10.1029/TR019i001p00505>
- Lewis, D.W. (1984). Practical sedimentology. Hutchinson Ross Publishing Company, Strousburg.
- Mange, M.A. and Maurer, H.F.W. (1992). Heavy minerals in colour. Chapman and Hall, London.
- Maya, K., Babu, K.N., Padmalal, D. and Seralathan, P. (2007). Hydrochemistry and dissolved nutrient flux of two small catchment rivers, south-western India. *Chem. Ecol.*, v.23, pp.13–27. <https://doi.org/10.1080/02757540601084029>
- Maya, K., Padmalal, D., Vandana, M., Mohan, S.V., Vivek, V.R., Limaye, R.B. and Kumaran K.P.N. (2022). Holocene changes in fluvial geomorphology, depositional environments, and evolution of coastal wetlands—A multiproxy study from Southwest India. In: K.P.N. Kumaran and D. Padmalal (Eds.), *Holocene Climate Change and Environment*, Elsevier, pp. 483–513. <https://doi.org/10.1016/B978-0-323-90085-0-00026-7>
- Mereena, C.S. and Prasad, T.K. (2020). The linkage between physical geographical conditions and mode of transportation: A case study from Alappuzha and Kottayam districts, Kerala. *Geo Eye*, v.9, pp.26–31. <https://doi.org/10.53989/bu.ge.v9i2.5>
- Najeeb, K. Md. (1999). Ground Water Exploration in Kerala Region as on

- 31-3-1999, Central Ground Water Board, Kerala Region, Trivandrum (Unpublished Report).
- Nair, K.M. and Rao, M.R. (1980). Stratigraphic analysis of Kerala basin, in: Proceedings of Symposium of Geological Survey and Geomorphology of Kerala. Geol. Surv. India, pp.1–8.
- Nair, K.M., Padmalal, D. and Kumaran, K.P.N. (2006). Quaternary geology of South Kerala sedimentary basin—an outline. Jour. Geol. Soc. India, v.67, pp.165–179.
- Nair, K.M. and Kumaran, K.P.N. (2006). Effects of Holocene climatic and sea level changes on ecology, vegetation and landforms in coastal Kerala. Project Completion Report, Kerala State Council for Science, Technology and Environment, Thiruvananthapuram.
- Narayana, A.C. and Priju, C.P. (2006). Evolution of coastal landforms and sedimentary environments of the late quaternary period along central Kerala, southwest coast of India. Jour. Coast. Res., v.39, pp.1898–1902. <https://www.jstor.org/stable/25743091>
- Nasir, U.P. and Harikumar, P.S. (2012). Hydrochemical and isotopic investigation of a tropical wetland system in the Indian subcontinent. Environment. Earth Sci., v.66, pp.111–119. <https://doi.org/10.1007/s12665-011-1211-9>
- Padmalal, D. and Seralathan, P. (1995). Geochemistry of Fe and Mn in surficial sediments of a tropical river and estuary, India—a granulometric approach. Environment. Geol., v.25, pp.270–276. <https://doi.org/10.1007/BF00766757>
- Padmalal, D., Maya, K. and Seralathan, P. (1997). Geochemistry of Cu, Co, Ni, Zn, Cd and Cr in the surficial sediments of a tropical estuary, southwest coast of India: a granulometric approach. Environment. Geol., v.31, pp.85–93. <https://doi.org/10.1007/s002540050167>
- Padmalal, D., Kumaran, K.P.N., Nair, K.M., Limaye, R.B., Mohan, S.V., Baijulal, B. and Anooja, S. (2014a). Consequences of sea level and climate changes on the morphodynamics of a tropical coastal lagoon during Holocene: An evolutionary model. Quarter. Internat., v.333, pp.156–172. <https://doi.org/10.1016/j.quaint.2013.12.018>
- Padmalal, D., Maya, K., Mohan, S.V. and Baburaj, B. (2014b). Holocene land-sea interactions and landform changes in the coastal lands of Vembanad lagoon, Kerala, SW India. Indian Jour. Geo-Mar. Sci., v.43, pp.1152–1156.
- Padmalal, D., Limaye, R.B. and Kumaran, K.P.N. (2022). Holocene climate and sea-level changes and their impact on ecology, vegetation and landforms in South Kerala Sedimentary Basin, India. In: K.P.N. Kumaran and D. Padmalal (Eds.), Holocene Climate Change and Environment. Elsevier, pp. 163–196. <https://doi.org/10.1016/B978-0-323-90085-0.00010-3>
- Passega, R. (1957). Texture as characteristic of clastic deposition. AAPG Bulletin, v.41, pp.1952–1984. <https://doi.org/10.1306/0BDA594E-16BD-11D7-8645000102C1865D>
- Passega, R. (1964). Grain size representation by CM patterns as a geologic tool. Jour. Sediment. Res., v.34, pp.830–847. <https://doi.org/10.1306/74D711A4-2B21-11D7-8648000102C1865D>
- Pejrup, M. (1988). The triangular diagram used for classification of estuarine sediments: a new approach. In: P.L. Boer, A. Van Gelder, and S.D. Nio (Eds.), Tide-influenced sedimentary environments and facies. Reidel, Dordrecht, pp. 289–300.
- Picard, M.D. (1971). Classification of fine-grained sedimentary rocks. Jour. Sediment. Res., v.41, pp.179–195. <https://doi.org/10.1306/74D7221B-2B21-11D7-8648000102C1865D>
- Pradhan, U.K., Sahoo, R.K., Pradhan, S., Mohany, P.K. and Mishra, P. (2020). Textural analysis of coastal sediments along East Coast of India. Jour. Geol. Soc. India, v.95, pp.67–74. <https://doi.org/10.1007/s12594-020-1387-2>
- Prahraj, P., Rekha, S. and Bhattacharya, A. (2021). Structure and chronology across the Achankovil terrain boundary shear zone system (South India), and its Madagascar connection in the Gondwanaland. Internat. Jour. Earth Sci., v.110, pp.1545–1573. <https://doi.org/10.1007/s00531-021-02029-5>
- Raj, D. and Shaji, E. (2017). Fluoride contamination in groundwater resources of Alleppey, southern India. Geosci. Front., v.8, pp.117–124. <https://doi.org/10.1016/j.gsf.2016.01.002>
- Sajeev, S., Sekar, S., Kumar, B., Senapathi, V., Chung, S. Y. and Gopalakrishnan, G. (2020). Variations of water quality deterioration based on GIS techniques in surface and groundwater resources in and around Vembanad Lake, Kerala, India. Geochemistry, v.80, pp.125626. <https://doi.org/10.1016/j.chemer.2020.125626>
- Shaji, J., Banerji, U.S., Maya, K., Joshi, K.B., Dabhi, A.J., Bharti, N. and Padmalal, D. (2022). Holocene monsoon and sea-level variability from coastal lowlands of Kerala, SW India. Quatern. Internat., v.642, pp.48–62. <https://doi.org/10.1016/j.quaint.2022.03.005>
- Shimizu, H., Tsunogae, T. and Santosh, M. (2009). Spinel+ quartz assemblage in granulites from the Achankovil Shear Zone, southern India: implications for ultrahigh-temperature metamorphism. Jour. Asian Earth Sci., v.36, pp.209–222. <https://doi.org/10.1016/j.jseaes.2009.06.005>
- Soman, K. (2002). Geology of Kerala. Geological Society of India Publication, Bangalore.
- Sundar, P.K.S. and Kundapura, S. (2023). Spatiotemporal variation in the water quality of Vembanad Lake, Kerala, India: a remote sensing approach. Environment. Monitor. Assess., v.195, pp.1097. <https://doi.org/10.1007/s10661-023-11746-0>
- Tessier, A.P.G.C., Campbell, P.G. and Bisson, M.J.A.C. (1979). Sequential extraction procedure for the speciation of particulate trace metals. Analyt. Chem., v.51, pp.844–851. <https://doi.org/10.1021/ac50043a017>
- Vaz, G.G., Mohapatra, G.P. and Hariprasad, M. (2002). Geomorphology and evolution of barrier-Lagoon coast in a part of north Andhra Pradesh. Geol. Soc. India, v.49, pp.30–40.
- Vikas, M. and Dwarakish, G.S. (2015). Coastal Pollution: A review. Aquat. Proced., v.4, pp. 381 –388. <https://doi.org/10.1016/j.aqpro.2015.02.051>